

# Fragmentation of 1.2A GeV/c $^{10}\text{C}$ in nuclear emulsion

**Bekmirzaev Rahmatulla Nurmuradivich-prof, Ulasheva Mashhura-student, Abduvaxabov Xondamir- student, Bahodir Nabiyeu -magistr**  
Jizzakh State Pedagogical Institute, Uzbekistan.  
e-mail:bekmirzaev@mail.ru

**Abstract.** It is discussed the experimental results and their comparison with multi-source thermal model calculations by fragmentation of isotope  $^{10}\text{C}$  to much lighter nuclear such as  $^8\text{Be}$ ,  $^4\text{He}$  and etc. Conclusions obtained basing on investigation and angle distribution analysis fragments relative direction projectile particles and also spectrum of distribution on transverse momentum of fragments from  $^{10}\text{C}$  allows possibility of using multi-source thermal model at energy of interactions 1.2 A GeV.

**Key words:** fragmentation, relativistic nuclei, model, emulsion, experiment, angle, momentum.

\*\*\*

## **Фрагментация $^{10}\text{C}$ в ядерной эмульсии при 1.2A GeV/c**

**Аннотация.** Обсуждаются экспериментальные результаты и их сравнение с расчетами термической модели многих источников по фрагментации изотопа  $^{10}\text{C}$  на более лёгких ядер, как  $^8\text{Be}$ ,  $^4\text{He}$  и др. Выводы, полученную на основе исследований и анализа угловых распределений фрагментов, относительно направление ядро снаряда, а также спектров распределения по поперечным импульсам фрагментов от  $^{10}\text{C}$  позволяет возможным использование термической модели многих источников для описание взаимодействий при энергии 1.2A ГэВ.

**Ключевые слово:** фрагментация, релятивистские ядра, модель, эмульсия, эксперимент, угол, импульс.

\*\*\*

## **1.2A GeV/c лик $^{10}\text{C}$ ядросининг ядро эмульсиясида фрагментацияси**

**Аннотация.** Экспериментал натижалар мухокома килинади Обсуждаются экспериментальные результаты и их сравнение с расчетами термической модели многих источников по фрагментации изотопа  $^{10}\text{C}$  на более лёгких ядер, как  $^8\text{Be}$ ,  $^4\text{He}$  и др. Выводы, полученную на основе исследований и анализа угловых распределений фрагментов, относительно направление ядро снаряда, а также спектров распределения по поперечным импульсам фрагментов от  $^{10}\text{C}$  позволяет возможным использование термической модели многих источников для описание взаимодействий при энергии 1.2A ГэВ.

**Ключевые слово:** фрагментация, релятивистские ядра, модель, эмульсия, эксперимент, угол, импульс.

## **1. Introduction**

Dissociation of relativistic nuclei on heavy target nuclei induced in the diffraction of electromagnetic and nuclear interactions[1-2]. Due to a collimation of fragments of the projectile -nucleus, definition of interactions as peripheral is simplified by moving towards to energy from

above 1.2 A GeV.

Minimal perturbation of a projectile makes them the most valuable sample for nuclear cluster physics. Excitation energy of a fragment ensemble is estimated as  $Q = M^* - M$ , where  $M^*$  is the ensemble invariant mass and  $M$  – a projectile mass. The value  $M^*$  is defined as  $M^{*2} = (\sum P_j)^2 = \sum (P_i \cdot P_k)$ , where  $P_{i,k}$  are 4-momenta of the fragments. Assumption of projectile speed conservation by relativistic fragments is sufficient to compensate the lack of momentum measurements. Already it is established that final states of relativistic He fragments effectively correlate with the clustering in the nuclei  $^{12}C$  [3],  $^6Li$  [4], and  $^9Be$  [5]. The described approach is used in the BECQUEREL Project [6] to study the drip line nuclei  $^7Be$ ,  $^8B$ ,  $^9C$ ,  $^{10}C$ , and  $^{12}N$  by means emulsion stacks exposed to secondary beams of the JINR Nuclotron [1-6].

## 2. Experimental material and results

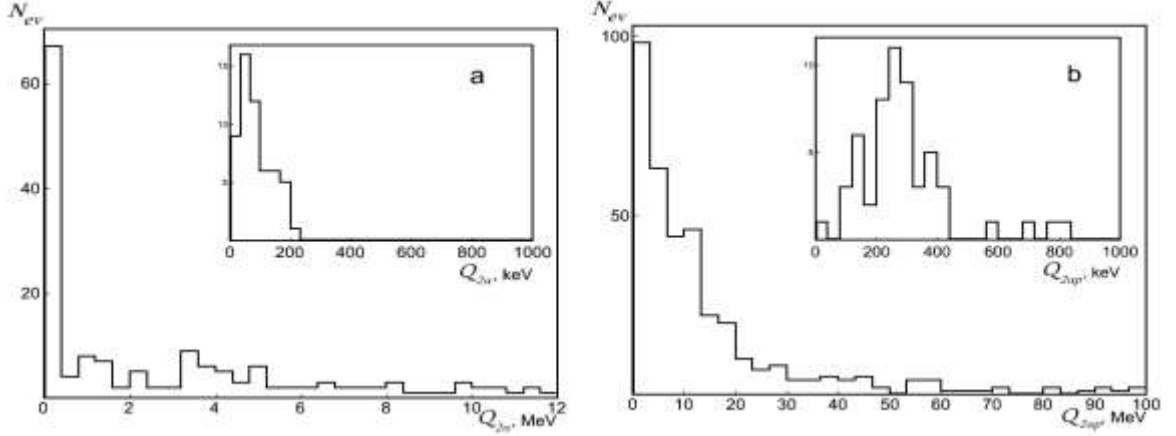
In table 1 shows distribution on channels dissociation numbers of "white" stars  $N_{ws}$  and events with fragments of a target or born mesons  $N_{tf}$ , for which the state  $Z_{pr} = \sum Z_{fr}$  and  $\sum Z_{fr} = 6$ . For a case  $\sum Z_{fr} = 6$  such state is checked up in 12 layers at calibration. The most probable channel is represented by 186 events  $2He + 2H$ , that it is followed expect for an isotope  $^{10}C$ . As an example on fig.2 is given the micrograph of the events of the nuclear fragmentation in the channel  $^{10}C \rightarrow 2\alpha + 2p$ .

Table 1. Distribution on channels dissociation numbers of "white" stars  $N_{ws}$  and events with fragments of a target or born mesons  $N_{tf}$ , for which satisfied state  $\sum Z_{fr} = 6$ .

Channel ( $^{10}C$ )	2He+2H	He+4H	3He	6H	Be+He	B+H	Li+3H	$^9C+n$
$N_{ws}=227$	186	12	12	9	6	1	1	-
100%	81.9	5.3	5.3	4.0	2.6	0.4	0.4	-
$N_{tf}=627$	361	160	15	30	17	12	2	30
100%	57.6	25.5	2.4	4.8	2.7	1.9	0.3	4.8

In the structure of the nucleus  $^{10}C$  basic role plays an unstable nucleus  $^8Be$ , which should occur in the dissociation of  $^{10}C \rightarrow ^8Be$ . Decays of relativistic nuclei  $^8Be \rightarrow 2\alpha$  via the ground state  $0^+$  is identified on an accessory  $\alpha$  - particle pairs to characteristic area of the least emission

angles  $\Theta_{2\alpha}$ , limited by an impulse 1.2 A GeV/c by a state  $\Theta_{2\alpha} < 10.5$  mrad.



**Fig. 1.** Distribution of the number of "white" stars  $N_{ws}$  of topology  $2\alpha + 2p$  on energy of excitation:  $Q_{2\alpha}$  pair  $\alpha$ -particles; on an insert - zoomed distribution of  $Q_{2\alpha}$  (a);  $Q_{2ap}$  triples  $2\alpha + p$ ; on an insert - zoomed distribution of  $Q_{2ap}$  (b).

As in the event of  ${}^9\text{Be} \rightarrow 8\text{Be}_{g.s.}$ , for 68 "white" stars  ${}^{10}\text{C} \rightarrow 2\alpha + 2p$  observed in  $\alpha$ -partial pair with emission angles do not exceed  $10^{-2}$  rad. Distribution of  $Q_{2\alpha}$  (Fig. 1a) suggests that in these events formed the nucleus  ${}^8\text{Be}_{g.s.}$ , that evidenced by the mean value for them  $\langle Q_{2\alpha} \rangle = (63 \pm 30)$  KeV for 83 keV RMS (in the inset in Fig. 1a). In turn, the distribution of  $Q_{2ap}$  (Fig. 1b) indicates that the dissociation of  ${}^{10}\text{C} \rightarrow 2\alpha + 2p$  accompanied by formation of an unbound nucleus  ${}^9\text{B}$ . The average value of  $\langle Q_{2ap} \rangle = (254 \pm 18)$  keV and 96 keV RMS (in the inset in Fig. 1b) are close to value of width and the energy decay of  ${}^9\text{B}_{g.s.} \rightarrow {}^8\text{Be}_{g.s.} + p$ . A clear correlation between the values of variables  $Q_{2\alpha}$  and  $Q_{2ap}$  for this group of events points to the cascade character of the process  ${}^{10}\text{C} \rightarrow {}^9\text{B} \rightarrow {}^8\text{Be}$ . It can be concluded that in the cluster structure of the nucleus  ${}^{10}\text{C}$  with a probability about  $(30 \pm 4)\%$  manifested nucleus  ${}^9\text{B}$ .

In favor of this statement evidenced by the distribution of the total transverse momentum of  $P_{T2ap}$  triples  $2\alpha + p$  from the "white" stars  ${}^{10}\text{C} \rightarrow {}^9\text{B}$  (Fig. 2). For a group of 40 events (73%) a value of  $\sigma_{PT}({}^9\text{B})$  amounts to  $(92 \pm 15)$  MeV/c, which corresponds to value 93 MeV/c, expected in the statistical model [7-8]. In this model, the radius of emission region the outside proton from the nucleus  ${}^{10}\text{C}$  is  $R_p = (2.3 \pm 0.4)$  Fermi, which is consistent with the value extracted from the data on the measurement of inelastic cross sections based model of the geometric overlap [6].

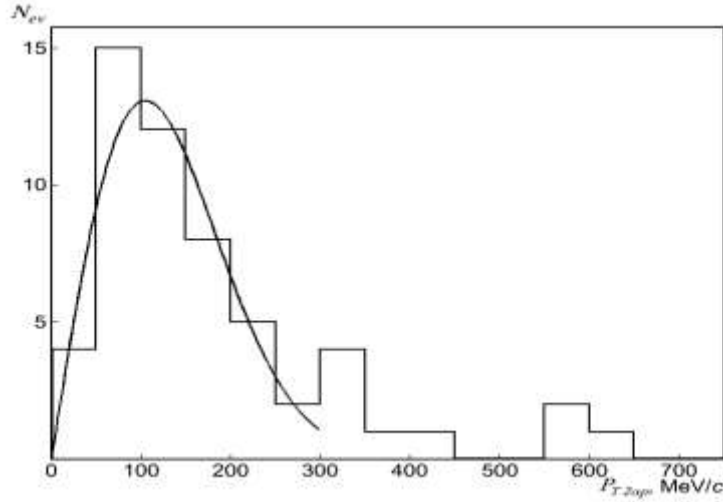


Fig. 2. The distribution of the total transverse momentum  ${}^9\text{B} \rightarrow 2\alpha + p$  (a), and distribution of the total transverse momentum  $2\alpha + 2p$  in the events  ${}^{10}\text{C} \rightarrow 2\alpha + 2p$  (b).

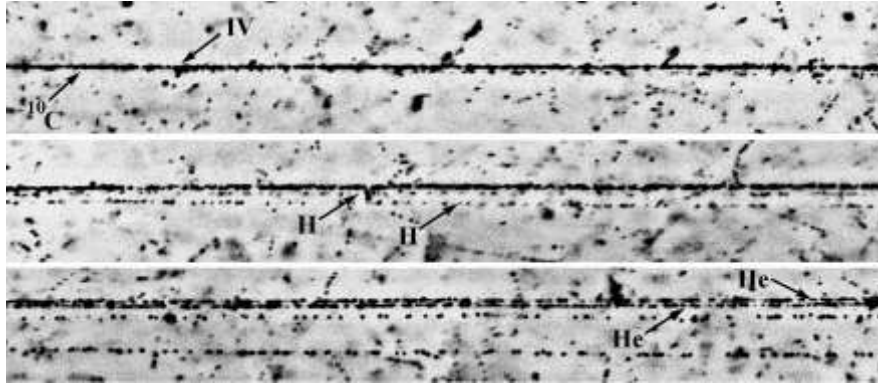


Fig. 3. Microphotograph of a «white» star  ${}^{10}\text{C} \rightarrow 2\text{He} + 2\text{H}$ . The interaction vertex is indicated as IV and secondary tracks are as H and He.

### 3. About model

We have used Liu's multisource thermal model [7-14] in this paper. According to the model, many emission sources are assumed to form in intermediate and high energy nucleus-nucleus collisions. Each source is assumed to emit produced particles or nuclear fragments.

In the rest frame of emission source for projectile fragments, we may treat the source as a classical ideal gas source due to low degree of excitation. Then, we have the Rayleigh distribution for transverse momentum ( $p'_T$ ) and Gaussian distribution for longitudinal momentum ( $p'_z$ ) [10-11]. Let  $\sigma$  denote the distribution width and  $R_{1,2,3}$  denote random numbers distributed evenly in  $[0, 1]$ , we have

$$p'_T = \sigma \sqrt{-2 \ln R} \quad (1)$$

$$p'_z = \sigma \sqrt{-2 \ln R_2} \cos(2\pi R_3) \quad (2)$$

where  $\sigma = \sqrt{mT}$ , and  $m$  and  $T$  are the fragment mass and source temperature respectively.

In the laboratory reference frame for projectile fragments, the transverse momentum ( $p_T$ ), longitudinal momentum ( $p_z$ ), and momentum ( $p$ ) can be given by

$$p_z = p'_z + \beta \quad (3)$$

$$p_T = p'_T \quad (4)$$

$$p = \sqrt{p_T^2 + p_z^2} \quad (5)$$

where  $B_z$  represents approximately the mean effect of Lorentz transformation and can be regarded as the source displacement [4,5]. The emission angle ( $\theta$ ) is given by

$$\theta = \arcsin\left(\frac{p_T}{p}\right) \approx \frac{p_T}{p} \approx \frac{p_T}{p_{\text{beam}}} \quad (6)$$

where  $p_{\text{beam}}$  denotes the beam momentum in unit of  $A$  GeV/c. Obviously,  $\theta$  has also the Rayleigh distribution.

Generally, nuclear fragments show a two-temperature emission. This indicates that we need a high temperature ( $T_H$ ) with a fraction of  $K$  and a low temperature ( $T_L$ ) with a fraction of  $1-K$  to describe the experimental data. The free parameters in the model are  $T_H$ ,  $T_L$ ,  $K$ , and  $B_z$ . If we do not care the momentum distribution, the parameter  $B_z$  may not be considered.

#### 4. Comparisons with model calculations

Figure 4 shows the distribution of the angle ( $\theta_{\alpha p}$ ) between the pair of fragments  $\alpha$  and  $p$  in  $^{10}\text{C}$  fragmentation in nuclear emulsion at 1.2A GeV/c. The histograms and curves are our experimental data and modeling results respectively. Especially, the dashed histogram and corresponding curve are for the process of  $^9\text{B} \rightarrow 2\alpha + p$  in dissociation of  $^{10}\text{C} \rightarrow ^9\text{B} + p \rightarrow 2\alpha + 2p$ . In the calculation, we have used a two-temperature emission picture with  $T_H = 24.85$  MeV,  $T_L = 1.14$  MeV, and  $K = 0.75$ . One can see that the model describes

approximately the experimental data.

The angular ( $\theta$ ) distributions of fragments emitted in the “white stars” for channel  $^{10}\text{C} \rightarrow 2\text{He} + 2\text{H}$  are shown in Figure 5. The histograms and curves are our experimental data and modeling results respectively. Especially, the dashed histogram and corresponding curve are for the isotopes of H, and the solid ones are for He fragments. In the calculation, we take  $T_H = 5.00$  MeV,  $T_L = 0.80$  MeV, and  $K = 0.70$  for the isotopes of H; and  $T_H = 8.33$  MeV,  $T_L = 1.25$  MeV, and  $K = 0.50$  for He fragments.

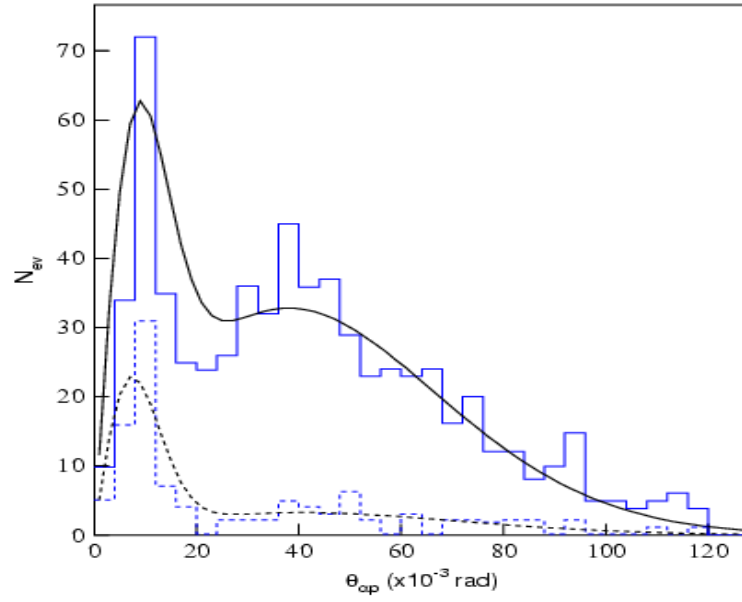


Figure 4. The distribution of the angle  $\theta_{\alpha p}$  between the pair of fragments  $\alpha$  and  $p$  in  $^{10}\text{C}$  fragmentation in nuclear emulsion at  $1.2A$  GeV/ $c$ . The histograms and curves are our experimental data and modeling results respectively.

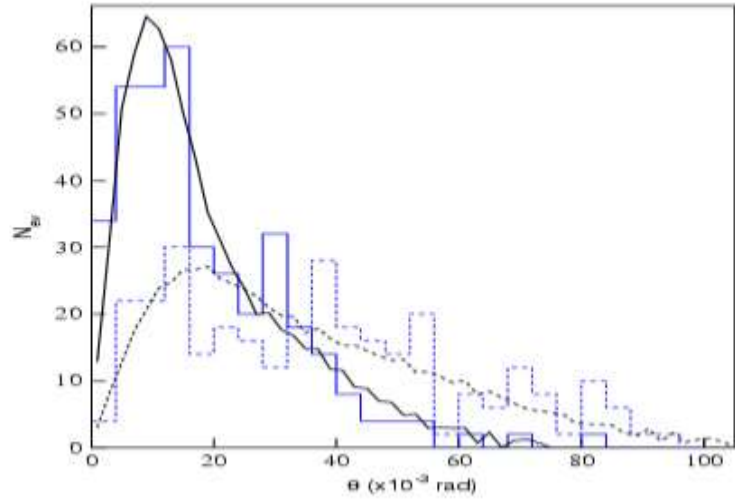


Figure 5. The angular ( $\theta$ ) distributions of fragments emitted in the “white stars” for channel  $^{10}\text{C} \rightarrow 2\text{He} + 2\text{H}$ . The notation is identical to that fig.4

The distributions of magnitudes  $p\beta c$  for H from  $^{10}\text{C} \rightarrow 2\text{He} + 2\text{H}$ ,  $^3\text{He}$  from  $^9\text{C}$  in  $^{10}\text{C} \rightarrow ^9\text{C} + n$ , and  $^4\text{He}$  from  $^{10}\text{C} \rightarrow 2\text{He} + 2\text{H}$  are displayed in Figure 6 by the solid, dotted, and dashed histograms (experimental data) and curves (modeling results), respectively. During the calculations was obtained following values of parameters for above mentioned events:  $T_H = T_L = 0.068$  GeV and  $B_z = 1.23$  GeV/c for H,  $T_H = T_L = 0.089$  GeV and  $B_z = 4.74$  GeV/c for  $^3\text{He}$ , and  $T_H = T_L = 0.125$  GeV and  $B_z = 7.24$  GeV/c for  $^4\text{He}$ , respectively. We see that there is no differences between the two sources for the distributions of  $p\beta c$ . In fact, we have used a single source to give a description for the distribution.

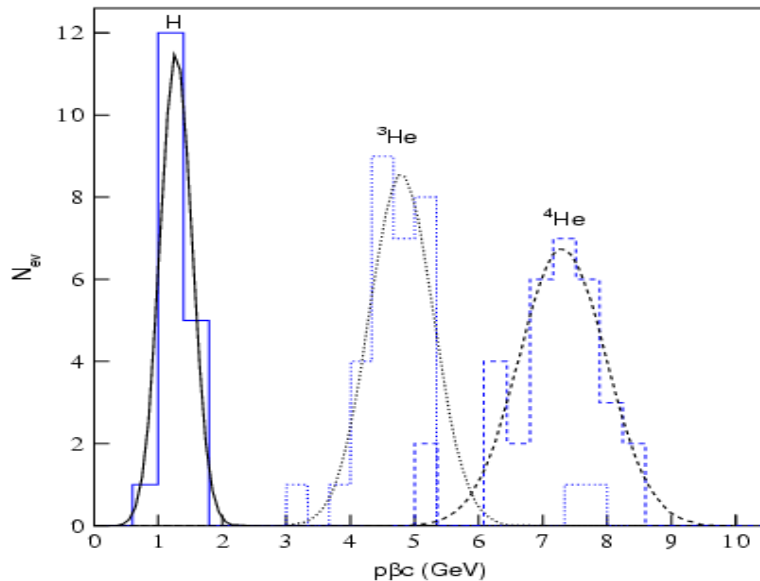


Figure 6. The distributions of magnitudes  $p\beta c$  for H from

$^{10}\text{C} \rightarrow 2\text{He} + 2\text{H}$ ,  $^3\text{He}$   $^9\text{C}$  in  $^{10}\text{C} \rightarrow ^9\text{C} + \text{n}$ , and  $^4\text{He}$  from  $^{10}\text{C} \rightarrow 2\text{He} + 2\text{H}$ .

The notation is identical to that fig.4

The distributions of  $p\beta c$  for  $^3\text{He}$  from  $^{10}\text{C} \rightarrow 2\ ^3\text{He} +\ ^4\text{He}$ ,  $^3\text{He}$  from  $^{10}\text{C} \rightarrow\ ^7\text{Be} +\ ^3\text{He}$ , and  $^4\text{He}$  from  $^{10}\text{C} \rightarrow 2\ ^3\text{He} +\ ^4\text{He}$  are displayed in Figure 7 by the solid, dotted, and dashed histograms (experimental data) and curves (modeling results), respectively. In the calculation, we have  $T_H = T_L = 0.157\ \text{GeV}$  and  $B_z = 4.26\ \text{GeV}/c$  for  $^3\text{He}$  from  $^{10}\text{C} \rightarrow 2\ ^3\text{He} +\ ^4\text{He}$ ,  $T_H = T_L = 0.157\ \text{GeV}$  and  $B_z = 4.62\ \text{GeV}/c$  for  $^3\text{He}$  from  $^{10}\text{C} \rightarrow\ ^7\text{Be} +\ ^3\text{He}$ , and  $T_H = T_L = 0.100\ \text{GeV}$  and  $B_z = 7.44\ \text{GeV}/c$  for  $^4\text{He}$ , respectively. We see again that a single source describes the distributions of  $p\beta c$ . Once more the model describes approximately the experimental data.

The transverse momentum ( $p_{T2\alpha 1p}$ ) distribution of total  $2\alpha + 1p$  from  $^{10}\text{C} \rightarrow 2\alpha + 2p$  is given in Figure 8. The histogram and curve are our experimental data and modeling results respectively. According to the conservation of momentum,  $p_{T2\alpha 1p} = p_{T1p}$  which is the transverse momentum of the last proton. In the calculation, we take  $T_H = 39.60\ \text{MeV}$ ,  $T_L = 6.45\ \text{MeV}$ , and  $K = 0.50$ . The analysis of transverse momentum spectrum for investigation events shows that in a field of  $p_t \approx 100\ \text{MeV}/c$  it has little deviation from experimental results.



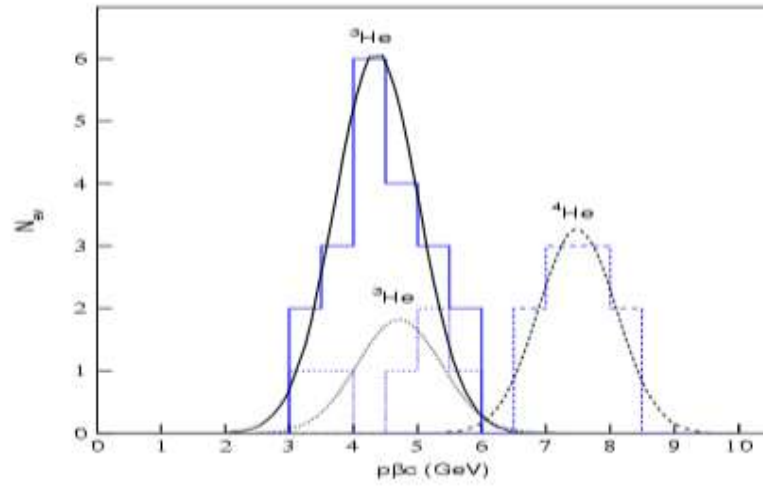


Figure 7. The distributions of  $p\beta c$  for  ${}^3\text{He}$  from  ${}^{10}\text{C} \rightarrow 2 {}^3\text{He} + \text{He}$ ,  ${}^3\text{He}$  from  ${}^{10}\text{C} \rightarrow {}^7\text{Be} + {}^3\text{He}$ , and  ${}^4\text{He}$  from  ${}^{10}\text{C} \rightarrow 2 {}^3\text{He} + {}^4\text{He}$ . The notation is identical to that fig.4

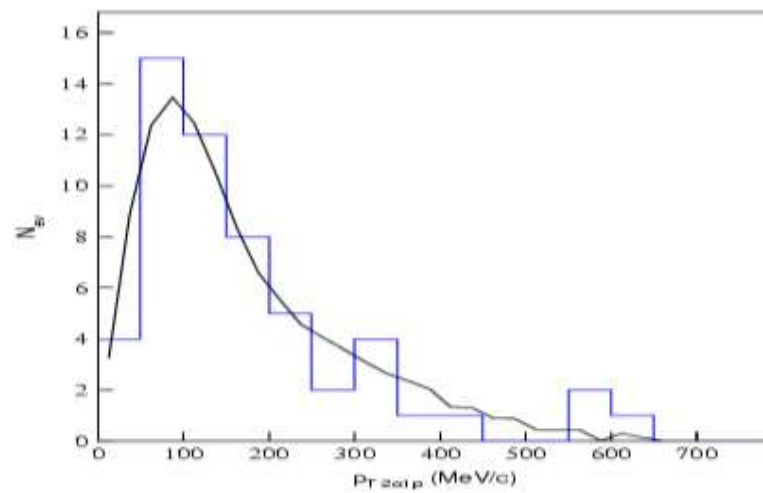


Figure 8. The transverse momentum ( $p_{T2\alpha 1p}$ ) distribution of total  $2\alpha+1p$  from  ${}^{10}\text{C} \rightarrow 2\alpha+2p$ . The histogram and curve are our experimental data and modeling results respectively.

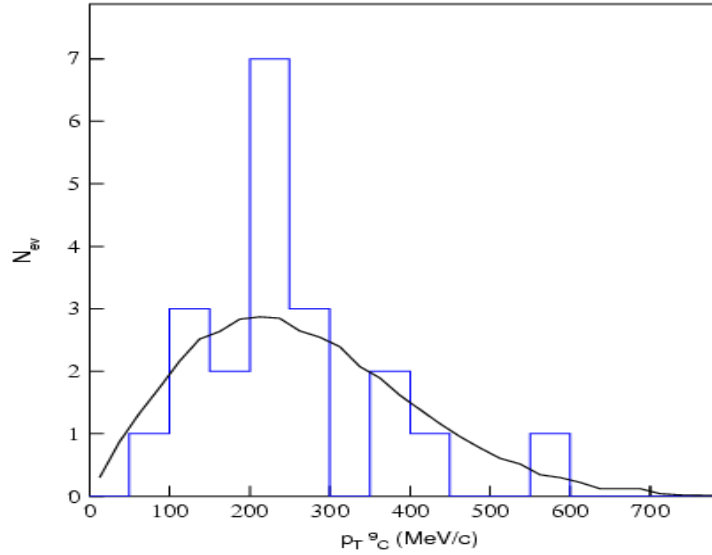


Figure 9. The transverse momentum ( $p_{T}^{9C}$ ) distribution of  ${}^9C$  from  ${}^{10}C \rightarrow {}^9C+n$ .

The notation is identical to that fig.4

The transverse momentum ( $p_{T}^{9C}$ ) distribution of  ${}^9C$  from  ${}^{10}C \rightarrow {}^9C+n$  is given in Figure 9. The histogram and curve are our experimental data and modeling results respectively. In the calculation, we take  $T_H = T_L = 48.00$  MeV. Once more the model describes approximately the experimental data.

### Conclusion

The distribution of the angle ( $\theta_{\alpha p}$ ) between the pair of fragments  $\alpha$  and p in  ${}^{10}C$  fragmentation in nuclear emulsion at 2A GeV/c has been obtained in the framework of Liu's multi-source thermal model. We have found the Rayleigh distribution for transverse momentum ( $p_T$ ) and Gaussian distribution for longitudinal momentum ( $p_z$ ) according the above mentioned model.

## References

1. N. P. Andreeva et al., Phys. Atom. Nucl. 68, 455(2005); nucl-ex/0605015.
2. M. I. Adamovich et al., Phys. Atom. Nucl. 62, 1378 (1999).
3. V. V. Belaga et al., Phys. Atom. Nucl. 58, 1905(1995).
4. D. A. Artemenkov et al., Phys. Atom. Nucl. 70, 1226 (2007); nucl-ex/0605018.
5. P. A. Rukoyatkin et al.: Secondary nuclear fragment beams for investigations of relativistic fragmentation of light radioactive nuclei using nuclear photoemulsion at Nuclotron. Eur. Phys. J. ST 162, 267 (2008).
6. The BECQUEREL Project, <http://becquerel.jinr.ru/>.
7. F. H. Liu and Y. A. Panebratsev, Phys. Rev. C **59**, 1193 (1999)
8. F. H. Liu and Y. A. Panebratsev, Phys. Rev. C **59**, 1798 (1999)
9. M. I. Adamovich et al., Phys. Atom. Nucl. 62, 1378 (1999).
10. F. H. Liu, J. S. Li, Phys. Rev. C **78**, 044602 (2008)
11. F. H. Liu, Phys. Rev. C **69**, 067901 (2004)
12. F. H. Liu, N. N. Abd Allah, B. K. Singh, Phys. Rev. C **69**, 057601 (2004)
13. F. H. Liu and Y. A. Panebratsev, Nucl. Phys. A **641**, 379 (1998)
14. F. H. Liu, Phys. Lett. B **583**, 68 (2004)